J-PARC-TH-0220

Pileup corrections on higher-order cumulants

Toshihiro Nonaka,[1, *] Masakiyo Kitazawa,[2, 3, †] and ShinIchi Esumi[1, ‡]

[1] *Tomonaga Center for the History of the Universe, University of Tsukuba, Tsukuba, Ibaraki 305, Japan*
[2] *Department of Physics, Osaka University, Toyonaka, Osaka 560-0043, Japan*
[3] *J-PARC Branch, KEK Theory Center, Institute of Particle and Nuclear Studies, KEK, 203-1, Shirakata, Tokai, Ibaraki, 319-1106, Japan*

We propose a method to remove the contributions of pileup events from higher-order cumulants and moments of event-by-event particle distributions. Assuming that the pileup events are given by the superposition of two independent single-collision events, we show that the true moments in each multiplicity bin can be obtained recursively from lower multiplicity events. In the correction procedure the necessary information are only the probabilities of pileup events. Other terms are extracted from the experimental data. We demonstrate that the true cumulants can be reconstructed successfully by this method in simple models. Systematics on trigger inefficiencies and correction parameters are discussed.

arXiv:2006.15809v1 [physics.data-an] 29 Jun 2020

I. INTRODUCTION

One of the ultimate goals of high energy physics experiments is to study the Quantum Chromo-Dynamics (QCD) phase diagram and especially the search for the QCD critical point [1]. It was suggested that the higher-order fluctuation observables are sensitive to the critical point, and the phase transition from quark-gluon plasma phase to the hadron-gas phase [2–5]. There have been lots of experimental efforts to measure the higher-order cumulants of event-by-event net-particle distributions such as net-proton, net-charge and net-kaon multiplicity distributions reported by ALICE [6], HADES [7], NA61 [8] and STAR collaborations [9–14]. In particular, the ratio of fourth to the second order cumulants of the net-proton distributions were presented to behave nonmonotonically as a function of collision energy with a strong enhancement at $\sqrt{s_{\rm NN}} = 7.7$ GeV [13]. This result is qualitatively similar to a theoretical model prediction [15], which would imply the existence of the critical point at low collision energy region. In order to establish the signal from the critical point, it is important to investigate further lower collision energy region, where the signal is predicted to decrease again [15]. Such experiments are being carried out by the STAR collaboration with the fixed-target mode instead of the collider mode at RHIC. In addition, future facilities focusing on low collision energies $\sqrt{s_{\rm NN}} <10$ GeV like CBM [16] and J-PARC-HI [17] experiments are also going to run with fixed-target mode.

One major issue expected in fixed-target experiments is pileup events. When two collision events occur on the target within a small space and and time interval, they are identified as a single event. These events are called the pileup event. Usually, the rate of the pileup events is well suppressed and the effect is negligible for most of the measurements. Even if not, the effect would be removed from any averaged observables once the pileup probability is well understood and estimated. Unfortunately, this is not the case for the higher order fluctuation observables. It was pointed out that the pileup events lead to a strong enhancement of the fourth order cumulant and moment at central collisions [18, 19]. However, the correction method has not been known. Because the pileup events give rise to a fake enhancement, this effect makes it difficult to interpret the final results of the critical point search. In the future experiments at CBM and J-PARC-HI, a proper understanding of the pileup events will be more crucial, because high collision rates which will be achieved by these experiments would enhance the probability of the pileups. Development of a correction method are urgent for proper understanding of upcoming experimental results.

In the present work, we propose a method to correct higher-order moments and cumulants for the pileup effects. Assuming that the pileup events consist of independent single-collision events, we derive the relations to connect the experimentally-observed moments including the pileup effects with the true moments. We also propose a systematic procedure to obtain the true cumulants using these relations by a recursive reconstruction of moments from lower multiplicity events. We then demonstrate the validity of this method by applying it to simple models. Systematics on trigger inefficiencies and correction parameters are also discussed.

This paper is organized as follows. In Sec. II, we explain the methodology for pileup corrections and derive correction formulas. The method is demonstrated in Sec. III with the extreme cases and realistic situations. In Sec. IV we discuss systematics of our method. We then summarize this work in Sec. V.

---

[*] nonaka.toshihiro.ge@u.tsukuba.ac.jp

[†] kitazawa@phys.sci.osaka-u.ac.jp

[‡] esumi.shinichi.gn@u.tsukuba.ac.jp

II. METHODOLOGY

A. Pileup events

Let us first clarify the definition of the pileup events and assumptions to be made in the present study.

First, in experimental analyses the pileup events are removed using various methods, some of which are carried out by offline analysis. For example, suppose a correlation plot between number of particles measured by two detectors in different acceptances. The normal single-collision events are expected to appear as a band having a positive or negative slope. On the other hand, the pileup events would appear as additional bands having different slopes and/or offsets, while there could be be some uncorrelated components. The pileup events are then removed by cutting outlier events outside the correlated band. However, there will be a finite probability that the band is contaminated by the pileup events due to randomness. These events cannot be removed by this analysis. We call these residual events remaining after various cutting as the pile up events, and investigate the correction of their effects.

Second, in the following discussion two distribution functions play crucial roles. One of them is the "multiplicity distribution", i.e. the distribution of the number of produced particles measured at mid- or forward-rapidity. The multiplicity is sometimes used to define centrality. The other distribution is the "particle distribution". In the event-by-event analysis, we focus on the distribution of the number of a specific particle or charge, N, such as the net-proton number or net-charge, represented by the probability distribution function $P(N)$, and study its cumulants. Throughout this study, we consider the distribution of a single variable N to simplify the discussion, but it is straightforward to extend the following method to deal with the multi-particle distributions, $P(N_1, N_2, \cdots)$, and the mixed cumulants of various particle species.

The distribution $P(N)$ depends on the multiplicity. Throughout this paper, we denote the experimentally-observed distribution function including the pileup effects at multiplicity m as $P_m(N)$, while the distribution of N in true single-collision events are represented as $P_m^{\rm t}(N)$. We suppose that m and N would be measured at different acceptances to reduce the auto-correlation effects between m and N. This means that a collision event with $m = 0$ can take place and have with nonzero N.

Third, except for Sec. II C we consider the pileup events composed of two single-collision events. As discussed in Sec. II C, it is possible to extend the following analysis to include the pileup events with more than two single-collisions. The probability of those events, however, are usually well suppressed and explicit consideration of their effects are not needed. The important assumption taken throughout this paper is that two single-collision events included in a pileup event are independent.

B. Pileup correction

Let us suppose that the pileup events occur with the probability α_m at the mth multiplicity bin. Then, the probability to find N particles of interest at multiplicity m with the pileup effects is given by

$$P_m(N) = (1-\alpha_m)P_m^{\rm t}(N) + \alpha_m P_m^{\rm pu}(N), \tag{1}$$

where $P_m^{\rm t}(N)$ and $P_m^{\rm pu}(N)$ are the probability distribution functions of N for the true (single-collision) and pileup events, respectively. The pileup events are further decomposed into the "sub-pileup" events given by the superposition of two single-collision events with multiplicities i and j satisfying $m = i + j$ as

$$P_m^{\rm pu}(N) = \sum_{i,j} \delta_{m,i+j} w_{i,j} P_{i,j}^{\rm sub}(N), \tag{2}$$

$$P_{i,j}^{\rm sub}(N) = \sum_{N_i,N_j} \delta_{N,N_i+N_j} P_i^{\rm t}(N_i) P_j^{\rm t}(N_j), \tag{3}$$

where $P_{i,j}^{\rm sub}(N)$ represents the probability distribution of N in the sub-pileup events labeled by (i,j), and $w_{i,j}$ is the probability to observe the sub-pileup events among the pileup events at the mth multiplicity bin. The sum over i and j runs non-negative integers. Obviously $w_{i,j}$ satisfies $w_{i,j} = w_{j,i}$ and

$$\sum_{i,j} \delta_{m,i+j} w_{i,j} = 1. \tag{4}$$

From Eq. 4 one also finds $w_{0,0} = 1$.

The pileup probabilities α_m and $w_{i,j}$ are related to the multiplicity distribution of the single-collision events. Let $T(m)$ be the multiplicity distribution, i.e. probability that a collision event with multiplicity m occurs for all single-collision events. When all sub-pileup events are rejected by an experimental analysis with the same resolution, the probability to find a sub-pileup event labeled by (i,j) among all collision events is given by $\alpha T(i)T(j)$, where α denotes the probability to find a pileup event among all collision events. Also, the probability to find an event with multiplicity

m without distinction between single-collision and pileup events is given by $(1-\alpha)T(m)+\alpha\sum_{i,j}\delta_{m,i+j}T(i)T(j)$. We thus have

$$w_{i,j} = \frac{\alpha T(i)T(j)}{\sum_{i,j}\delta_{m,i+j}\alpha T(i)T(j)}, \tag{5}$$

$$\alpha_m = \frac{\alpha\sum_{i,j}\delta_{m,i+j}T(i)T(j)}{(1-\alpha)T(m)+\alpha\sum_{i,j}\delta_{m,i+j}T(i)T(j)}. \tag{6}$$

Therefore, in this case α_m and $w_{i,j}$ are completely determined from α and $T(m)$. We, however, note that Eqs. 5 and 6 might not hold in realistic experimental cases if the probability distribution of the pileup rejection is different from the multiplicity distribution. We thus do not use Eqs. 5 and 6 explicitly in the rest of this section. In real experiments, $w_{i,j}$ can directly be estimated by some reasonable assumptions within the experimental simulation. The models employed in Sec. III satisfy Eqs. 5 and 6.

From Eqs. 1, 2 and 3, the moment generating function [20] for events at multiplicity m is expressed as

$$\begin{aligned} G_m(\theta) &= \sum_N e^{N\theta}P_m(N) \\ &= (1-\alpha_m)G^{\rm t}_m(\theta) + \alpha_m\sum_{i,j}\delta_{m,i+j}w_{i,j}G^{\rm sub}_{i,j}(\theta), \end{aligned} \tag{7}$$

with

$$G^{\rm sub}_{i,j}(\theta) = G^{\rm t}_i(\theta)G^{\rm t}_j(\theta), \tag{8}$$

where $G^{\rm t}_m(\theta)=\sum_N e^{N\theta}P^{\rm t}_m(N)$ is the moment generating function of $P^{\rm t}_m(N)$. The rth order moment of the observed distribution $P_m(N)$ is then given by

$$\begin{aligned} \langle N^r\rangle_m &= \sum_N N^r P_m(N) = \frac{d^r}{d\theta^r}G(\theta)|_{\theta=0} \\ &= (1-\alpha_m)\langle N^r\rangle^{\rm t}_m + \alpha_m\sum_{i,j}\delta_{m,i+j}w_{i,j}\langle N^r\rangle^{\rm sub}_{i,j}, \end{aligned} \tag{9}$$

with $\langle N^r\rangle^{\rm t}_m = \sum_N N^r P^{\rm t}_m(N)$ and

$$\langle N^r\rangle^{\rm sub}_{i,j} = \sum_N N^r P^{\rm sub}_{i,j}(N) = \sum_{k=0}^{r}\binom{r}{k}\langle N^{r-k}\rangle^{\rm t}_i\langle N^k\rangle^{\rm t}_j. \tag{10}$$

The right-hand sides in Eq. 10 up to fourth order are written as

$$\langle N\rangle^{\rm sub}_{i,j} = \langle N\rangle^{\rm t}_i + \langle N\rangle^{\rm t}_j, \tag{11}$$

$$\langle N^2\rangle^{\rm sub}_{i,j} = \langle N^2\rangle^{\rm t}_i + \langle N^2\rangle^{\rm t}_j + 2\langle N\rangle^{\rm t}_i\langle N\rangle^{\rm t}_j, \tag{12}$$

$$\langle N^3\rangle^{\rm sub}_{i,j} = \langle N^3\rangle^{\rm t}_i + \langle N^3\rangle^{\rm t}_j + 3\langle N^2\rangle^{\rm t}_i\langle N\rangle^{\rm t}_j + 3\langle N\rangle^{\rm t}_i\langle N^2\rangle^{\rm t}_j, \tag{13}$$

$$\langle N^4\rangle^{\rm sub}_{i,j} = \langle N^4\rangle^{\rm t}_i + \langle N^4\rangle^{\rm t}_j + 4\langle N^3\rangle^{\rm t}_i\langle N\rangle^{\rm t}_j + 4\langle N\rangle^{\rm t}_i\langle N^3\rangle^{\rm t}_j + 6\langle N^2\rangle^{\rm t}_i\langle N^2\rangle^{\rm t}_j. \tag{14}$$

We note that Eq. 10 is alternatively expressed using cumulants in a compact form as [20]

$$\langle N^r\rangle^{\rm sub}_{i,j,{\rm c}} = \langle N^r\rangle^{\rm t}_{i,{\rm c}} + \langle N^r\rangle^{\rm t}_{j,{\rm c}}, \tag{15}$$

where $\langle N^r\rangle^{\rm sub}_{i,j,{\rm c}}$ and $\langle N^r\rangle^{\rm t}_{j,{\rm c}}$ are the cumulants of the sup-pileup and true distributions, respectively.

Substituting Eq. 10 into Eq. 9, one obtains formulas connecting $\langle N^r\rangle_m$ and $\langle N^r\rangle^{\rm t}_m$. It is notable that in these formulas the observed moment $\langle N^r\rangle_m$ is given by the combination of the true moments $\langle N^{r'}\rangle^{\rm t}_{m'}$ with $r'\le r$ and $m'\le m$.

The true moments $\langle N^r\rangle^{\rm t}_m$ are obtained from the observed moments $\langle N^r\rangle_m$ by solving Eqs. 9 and 10. This procedure can be carried out recursively starting from $m=0$ and $r=1$, and by increasing m and r. To see this, it is convenient to rewrite Eqs. 9 and 10 as

$$\langle N^r\rangle^{\rm t}_m = \frac{\langle N^r\rangle_m - \alpha_m C^{(r)}_m}{1-\alpha_m+2\alpha_m w_{m,0}}, \tag{16}$$

with

$$C^{(r)}_m = \mu^{(r)}_m + \sum_{i,j>0}\delta_{m,i+j}w_{i,j}\langle N^r\rangle^{\rm sub}_{i,j}, \tag{17}$$

and

$$\mu_m^{(r)} = \begin{cases} 2w_{m,0}\displaystyle\sum_{k=0}^{r-1}\binom{r}{k}\langle N^{r-k}\rangle_0^{\mathrm{t}}\langle N^k\rangle_m^{\mathrm{t}} & (m>0), \\ \displaystyle\sum_{k=1}^{r-1}\binom{r}{k}\langle N^{r-k}\rangle_0^{\mathrm{t}}\langle N^k\rangle_0^{\mathrm{t}} & (m=0). \end{cases} \tag{18}$$

Up to the fourth order, the explicit forms of $\mu_m^{(r)}$ are

$$\mu_m^{(1)} = 0, \tag{19}$$
$$\mu_m^{(2)} = 2w_{m,0}\left[\langle N^2\rangle_0^{\mathrm{t}} + 2\langle N\rangle_m^{\mathrm{t}}\langle N\rangle_0^{\mathrm{t}}\right], \tag{20}$$
$$\mu_m^{(3)} = 2w_{m,0}\left[\langle N^3\rangle_0^{\mathrm{t}} + 3\langle N^2\rangle_m^{\mathrm{t}}\langle N\rangle_0^{\mathrm{t}} + 3\langle N\rangle_m^{\mathrm{t}}\langle N^2\rangle_0^{\mathrm{t}}\right], \tag{21}$$
$$\mu_m^{(4)} = 2w_{m,0}\left[\langle N^4\rangle_0^{\mathrm{t}} + 4\langle N^3\rangle_m^{\mathrm{t}}\langle N\rangle_0^{\mathrm{t}} + 4\langle N\rangle_m^{\mathrm{t}}\langle N^3\rangle_0^{\mathrm{t}} + 6\langle N^2\rangle_m^{\mathrm{t}}\langle N^2\rangle_0^{\mathrm{t}}\right], \tag{22}$$

for $m > 0$ and

$$\mu_0^{(1)} = 0, \tag{23}$$
$$\mu_0^{(2)} = 2\langle N_0\rangle^{\mathrm{t}}\langle N_0\rangle^{\mathrm{t}}, \tag{24}$$
$$\mu_0^{(3)} = 6\langle N_0^2\rangle^{\mathrm{t}}\langle N_0\rangle^{\mathrm{t}}, \tag{25}$$
$$\mu_0^{(4)} = 8\langle N_0^3\rangle^{\mathrm{t}}\langle N_0\rangle^{\mathrm{t}} + 6\langle N_0^2\rangle^{\mathrm{t}}\langle N_0^2\rangle^{\mathrm{t}}. \tag{26}$$

To obtain the true moments $\langle N^r\rangle_m^{\mathrm{t}}$, we first use the fact that $C_0^{(1)} = 0$, which leads to $\langle N\rangle_0^{\mathrm{t}} = \langle N\rangle_0/(1+\alpha_0)$. Next, Eqs. 17 and 18 shows that the correction factors $C_0^{(r)}$ at $m = 0$ are given only by the moments $\langle N^{r'}\rangle_0^{\mathrm{t}}$ with $r' < r$. One thus can obtain $\langle N^r\rangle_0^{\mathrm{t}}$ recursively from lower order up to any higher orders. Similarly, one can obtain the true moments at multiplicity $m = 1$ from lower order moments up to any order using the fact that the correction factor $C_1^{(r)}$ consists of $\langle N^{r'}\rangle_{m'}^{\mathrm{t}}$ with $r' \le r$ and $m' \le m$. By repeating the same procedure one can obtain the true moments for all multiplicities.

An important remark here is that this procedure can be carried out in almost data-driven way. Only thing we need is the probabilities $w_{i,j}$ and α_m, which would be determined by simulations.

C. Pileups composed of more than two single-collision events

So far, we considered the pileup events composed of two single-collision events. It is not difficult to extend these results to include the pileup events composed of three single-collision events. In this case, Eq. 2 is modified as

$$P_m^{\mathrm{pu}} = \sum_{i,j}\delta_{m,i+j}w_{i,j}P_{i,j}^{\mathrm{sub}}(N) + \sum_{i,j,k}\delta_{m,i+j+k}w_{i,j,k}P_{i,j,k}^{\mathrm{sub}}(N), \tag{27}$$

where $P_{i,j,k}^{\mathrm{sub}}(N)$ represents the probability distribution of N on the sub-pileup events composed of three single collisions with multiplicities i, j, and k, and $w_{i,j,k}$ is the probability of the sub-pileup event. From the independence of the individual collisions, $P_{i,j,k}^{\mathrm{sub}}(N)$ is given by

$$P_{i,j,k}^{\mathrm{sub}} = \sum_{N_i,N_j,N_k}\delta_{N,N_i+N_j+N_k}P_i^{\mathrm{t}}(N_i)P_j^{\mathrm{t}}(N_j)P_j^{\mathrm{t}}(N_j). \tag{28}$$

Then, it is straightforward to derive the relations like Eqs. 9 and 16. These results allow us to obtain the true moments $\langle N^r\rangle_m^{\mathrm{t}}$ recursively from small m as before. In this way, pileups with arbitrary many single-collision events can be taken into account in principle.

III. MODEL

In this section we apply the procedure introduced in the previous section to the pileup correction in simple models and demonstrate that the true cumulants are successfully obtained.

A. Multiplicity distributions

Let us first generate a realistic multiplicity distribution with pileup events. We employ the Glauber and two-component model for this purpose. Two gold nuclei are collided in the Glauber model, where the *pp* cross section is chosen to be 33 mb. The number of participant nucleons, $N_{\rm part}$, and binary collisions, $N_{\rm coll}$, are obtained. In order to propagate $N_{\rm part}$ and $N_{\rm coll}$ to the multiplicity, we define the number of sources, $N_{\rm sc}$ as

$$N_{\rm sc} = (1-x)N_{\rm part} + xN_{\rm coll}, \tag{29}$$

where x is the fraction of the hard component. We choose $x = 0.1$ for the simulation. Particles are then generated from each source $N_{\rm sc}$ based on the negative binomial distribution:

$$P_{\mu,k}(N) = \frac{\Gamma(N+k)}{\Gamma(N+1)\Gamma(k)} \cdot \frac{(\mu/k)^N}{(\mu/k+1)^{N+k}}, \tag{30}$$

where μ is the mean value of particles generated from one source, and k corresponds to the inverse of width of the distribution. $\mu = 1.0$ and $k = 1.0$ are chosen for the simulation. In order to simulate the pileup events as well as normal single-collision events, multiplicities from two collision events are randomly superimposed with the probability $\alpha = 0.05$. In this way, 10 million Au+Au collision events are processed. We note that in this model the pileup probabilities $w_{i,j}$ and α_m are given by Eqs. 5 and 6 by construction.

The resulting multiplicity distribution is shown by the black line in Fig. 1. The blue squares show the multiplicity distribution from single-collision events, while those from pileup events are shown by the red circles. It is found that, due to the pileup events, the measured distribution has the tail on top of the distribution from the single-collision events. The inset panel shows α_m, i.e. the ratio of the pileup events at multiplicity m. From the panel one finds that α_m grows with increasing m. This behavior suggests that the effect of pileup events are more problematic in central collisions rather than peripheral collisions.

In Fig. 2, we plot the multiplicity distribution of single-collision events $T(m)$ and the number of sub-pileup events (i,j) normalized by total simulated events, $\alpha T(i)T(j)$. From these results $w_{i,j}$ and α_m are constructed according to Eqs. 5 and 6. These parameters are used in the following two subsections.

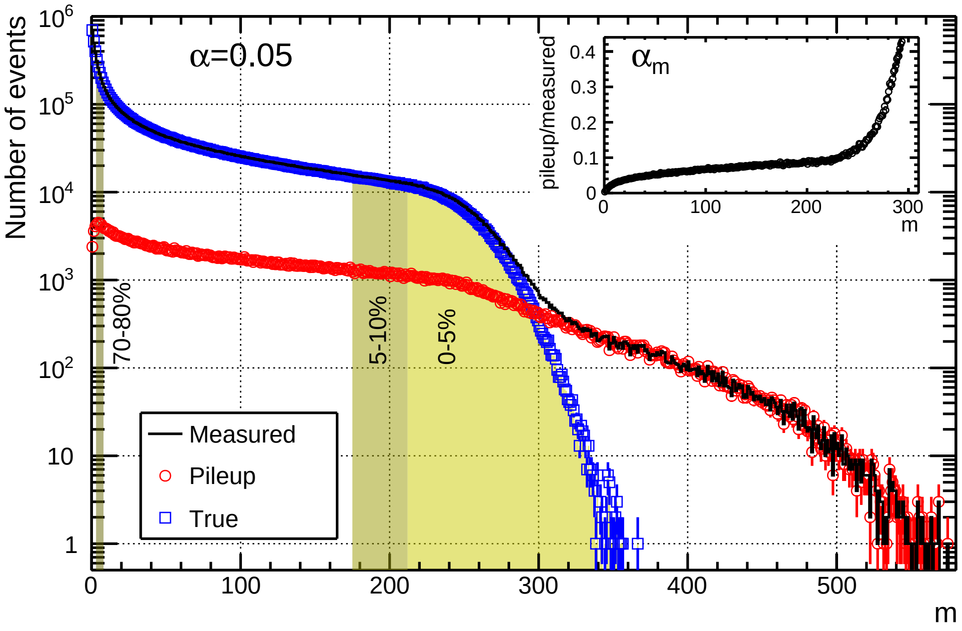

FIG. 1. The multiplicity distribution generated from the Glauber and two component model. The black line includes the contribution from pileup events with $\alpha = 0.05$ (measured distribution). The red open circles are the distribution from pileup events, and the blue squares are from the normal single collision events. The bands indicate 0-5%, 5-10% and 70-80% centralities. The inset panel shows the ratio of pileup to measured distributions as a function of multiplicity (α_m).

B. Simple case

In this and next subsections, we discuss the pileup correction for two model distributions $P^{\rm t}_m(N)$ with the multiplicity distribution obtained in Sec. III A. In this subsection, we consider a simple model where the particle number N obeys the Poisson distribution with the mean value of 10 at all the multiplicity bin. We emphasize that this model is totally impractical, because 10 particles on average are created at both $m = 0$ and $m = 300$. However, this model is suitable to demonstrate the validity of the recursive correction procedures. The more realistic model will be discussed in the next subsection.

Figure 3 shows the particle distribution for the first 4 multiplicity bins ($m = 0$, 1, 2, 3). The red circles show pileup events, and the blue squares show the single-collision events. The measured distribution given by the sum of these

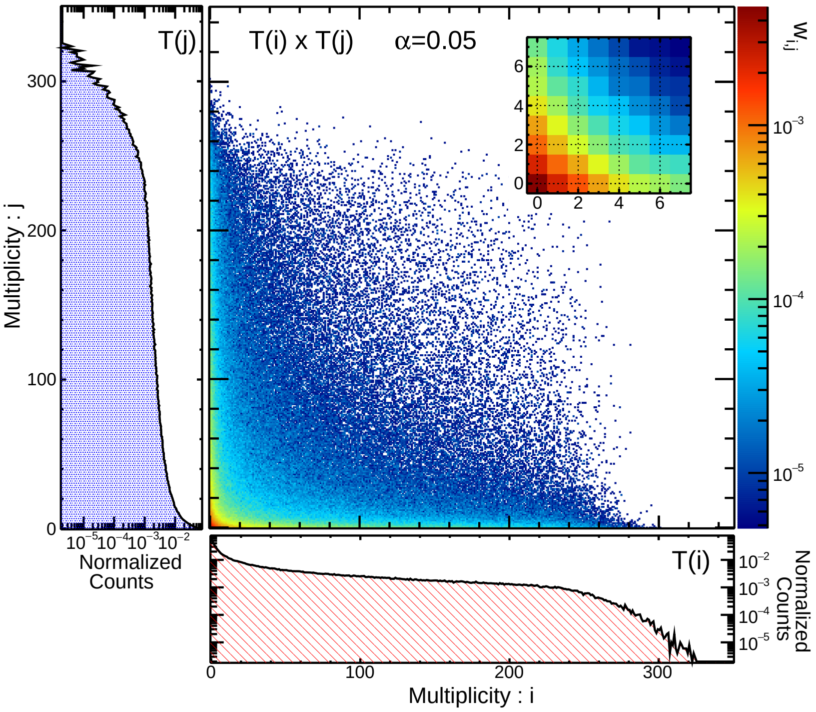

FIG. 2. Correlation between multiplicities i and j from two collisions which forms pileup events. Z-axis is normalized by total number of events. The inset panel shows the expanded plot at $x < 7$ and $y < 7$. Projected histograms into x and y axes are shown as well.

distributions is shown by the black solid lines, which are found to have a bump structure at $N \gtrsim 20$ due to pileup events. Other colored lines show the sub-pileup events for all possible combinations of (i,j) with $m = i+j$. In the case of $m = 0$, there is only one combination for sub-pileup, $(i, j) = (0, 0)$, and the distributions of pileup and sub-pileup events are identical and $w_{0,0} = 1$. As shown in Fig. 3 (b), (c) and (d), in the case of $m \geq 1$, the pileup distribution consists of multiple sub-pileup events with $(i, j) = (m, 0), \cdots, (0, m)$.

In Fig. 4, we show the cumulants $\langle N^r \rangle_{m,\mathrm{c}}$ at the mth multiplicity bin. In the figure, the cumulants are plotted for the true single-collision distribution obtained by the simulation, measured distribution with the pileup effects, and the corrected results. Statistical uncertainties are estimated by bootstrap. True cumulants are $\langle N^r_m \rangle = 10$ by definition. The measured cumulants have strong deviations from this value due to the pileup events [18, 19]. It is notable that the measured cumulants especially for $r = 1$ and 2 behave similar to what we have already seen in α_m in the inset panel in Fig. 1. Because the particles are generated according to the Poisson distributions having the same mean value, the effects from the pileup events only depend on the pileup probability. Corrected cumulants are found to be consistent with the true value $\langle N^r \rangle_{m,\mathrm{c}} = 10$ within statistics, which indicates that our method does work well. Large point-by-point variations are due to the increased statistical uncertainties after the corrections.

C. Realistic case

Next, we move on to more realistic case, where the mean value of N increases with increasing N_{part}. We again employ the Poisson distribution for N, but in contrast to the previous subsection we assume that the mean value varies depending on N_{part} as $\langle N \rangle = 0.05 N_{\mathrm{part}}$. We employ the same pileup probability $\alpha = 0.05$. The centrality is defined by dividing the multiplicity distribution of single-collision events (see Fig. 1 for corresponding regions in multiplicity distributions). Figure 5 shows the particle number distributions for 0-5%, 10-20%, 40-50% and 70-80% centralities. The pileup distributions are found inside the true distribution at peripheral collisions, while the pileup distributions in central collisions appear as a long tail in the measured distributions. Thus, large effects on cumulants are expected in central collisions in this simulation [19].

Cumulants for each multiplicity bin are averaged in each centrality by using event statistics as a weight [21], which are shown in Fig. 6 as a function of centrality. The centrality is $0-5\%$, $5-10\%$, $10-20\%$... ,$70-80\%$ from $x = 0$ to $x = 8$. In this case, significant deviation on measured cumulants are observed only in the central collisions, as was expected from Fig. 5. Corrected cumulants are consistent with true cumulants even at $0-5\%$. This result shows that the pileup correction proposed in Sec. II is successfully applicable to realistic particle distributions.

It would be interesting to discuss briefly about volume fluctuations [22]. In Fig. 6 the cumulants with fixed N_{part} are shown by the dotted lines. The difference between markers and lines seen especially for higher-order cumulants

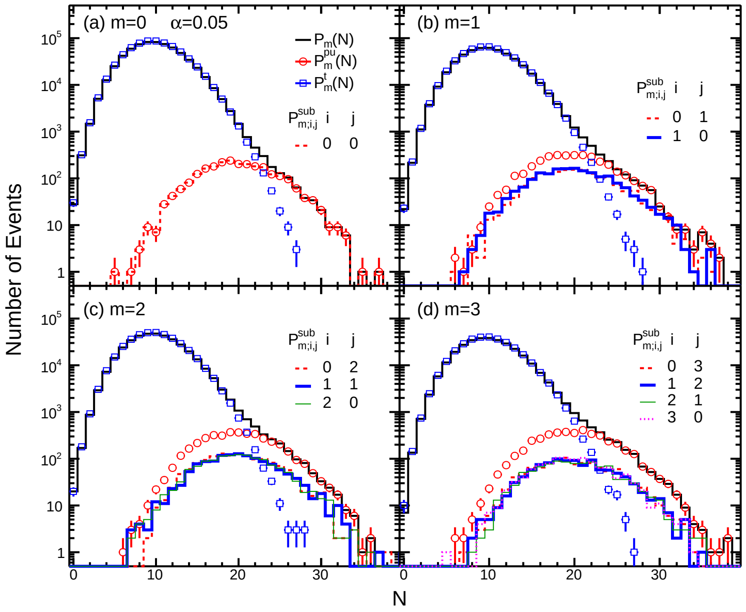

FIG. 3. Particle number distributions, $P_{m;i,j}(N)$, in the simple model in Sec. III B for the first 4 multiplicity bins, (a) $m = 0$, (b) $m = 1$, (c) $m = 2$ and (d) $m = 3$. The red circles shows the pileup events, and blue squares are for single-collision events. The black solid line is for measured events. Distributions for sub-pileups are shown in colored or dotted lines.

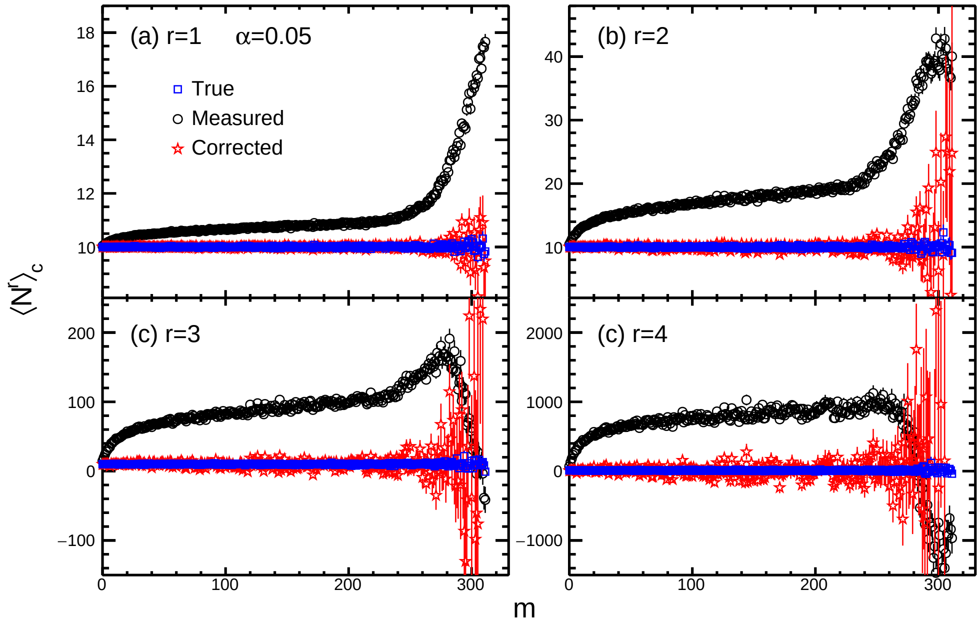

FIG. 4. Cumulants up to the 4th-order as a function of multiplicity in the simple model in Sec. III B. True values of cumulants are shown by the blue squares, and the measured value of cumulants (including pileup events) are shown by the black circles. The red stars show the results corrected for pileups.

indicate the residual volume (participant) fluctuations even after the centrality bin width averaging [21, 23]. This happens because we let $N_{\rm part}$ fluctuate event by event based on the Glauber model and the mean value of Poisson distribution is defined as the function of $N_{\rm part}$. It should be noted that the location of the kink structure at $x = 1 \sim 2$ (5-10% and 10-20% centralities), where the cumulants of $N_{\rm part}$ distribution have minimum or maximum values [23], observed in true and corrected cumulants would depend on the model and the binning of the centrality. Interestingly, the measured cumulants including pileup events look rather qualitatively normal (linear) compared to the true and corrected cumulants. This would imply that the pileup events could accidentally hide the characteristic kink structure arising from the volume fluctuations. One should always be careful if the effects from the volume fluctuations are removed from the measurements. Otherwise, the final results could be spoiled by sizable effects of both pileup and volume fluctuations.

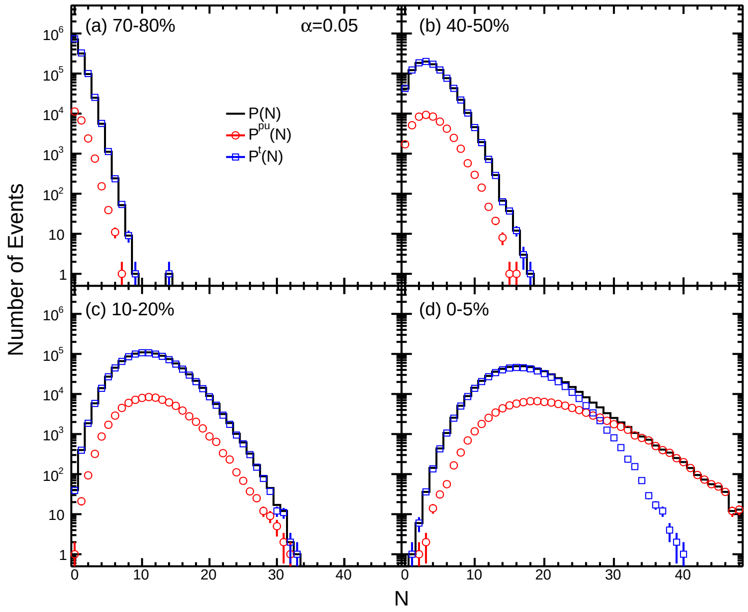

FIG. 5. Particle number distributions for (a) 70-80%, (b) 40-50%, (c) 10-20% and (d) 0-5% centralities in the realistic model in Sec. III C. The red circles shows the pileup events, and the blue squares are for single-collision events. The black solid line is for measured events.

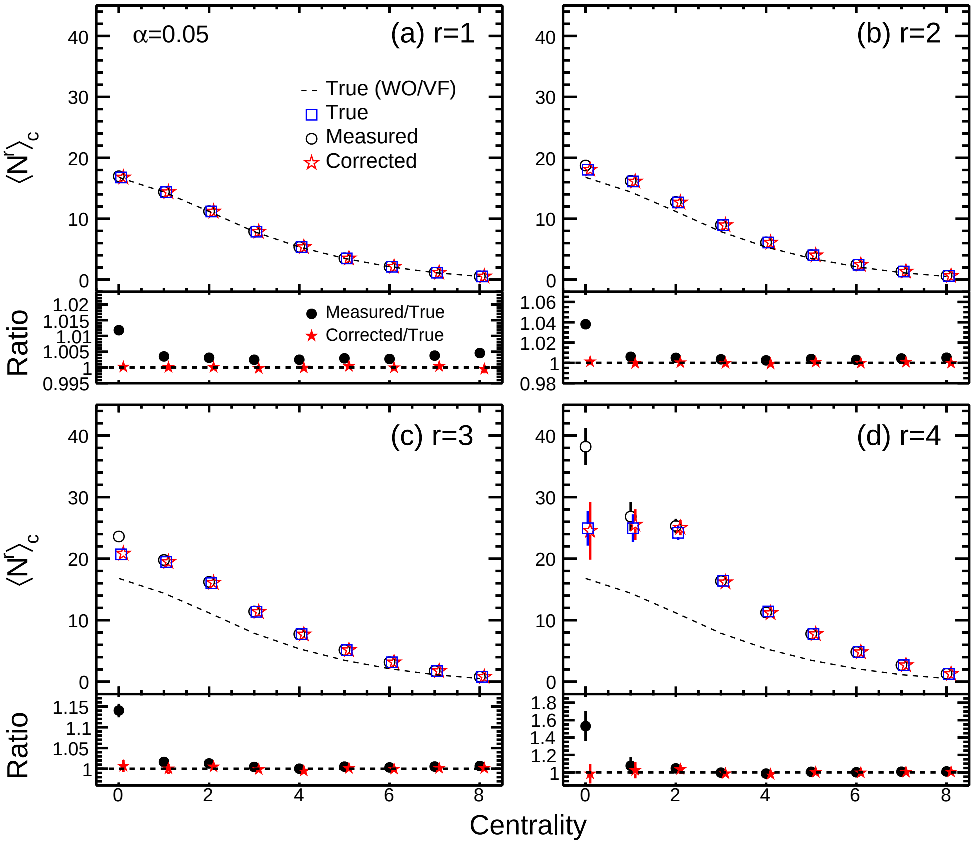

FIG. 6. Cumulants up to the 4th-order as a function of centrality, 0-5%, 5-10%, 10-20%, $\cdots$, and 70-80% centralities from $x = 0$ to 8. True values of cumulants are shown by the open blue squares, and the measured values of cumulants (including pileup events) are shown by open black circles. The red open stars show results corrected for pileups. The ratios of measured and corrected results to the true cumulants are shown by the filled markers in lower panels. The true values excluding volume fluctuations are shown in dotted lines.

IV. SYSTEMATICS

A. Trigger inefficiency

An important procedure of the pileup correction is the recursive solving of moments from the lowest multiplicity event at $m = 0$. At such super-peripheral collisions, however, the event itself cannot be triggered due to small multiplicity and the detector threshold to reject backgrounds. The event efficiency is thus reduced in peripheral collisions, which is known as "trigger inefficiency". It is possible that these effects at smaller multiplicity events accumulate in the recursive procedure and give rise to a large systematic deviation on the reconstructed cumulants at large m.

To check this problem, in this subsection the events for $m < 20$ are artificially reduced by the arbitrary function of the multiplicity, and the pileup correction is not applied for this region. In other words, we regard the observed moments $\langle N^r \rangle_m$ as the true moments $\langle N^r \rangle_m^{\rm t}$ for $m < 20$, and perform the correction only for $m \geq 20$. The model in Sec. III C is employed.

Figure 7 shows the ratios of measured and corrected cumulants to the true cumulants as a function of multiplicity. The averaged results for centrality bins 0-5, 5-10, 10-20, ... 50-60% are also shown. As the correction is not applied for $m < 20$, the corrected results are identical with measured values. On the other hand, the corrected cumulants for $m \geq 20$ are quickly approaching to the true value, which shows that the correction works well regardless of incorrect correction factors in peripheral collisions. This is because the sub-pileup moments (the second term in Eq. 9) have less contributions from peripheral collisions due to the tiny production rate of particles of interest. Since it depends on how significant the production of particles of interest is in peripheral collisions compared to central collisions, we would propose to check the results by changing the starting point of the recursive corrections, and implement it as a part of systematic uncertainties in final results.

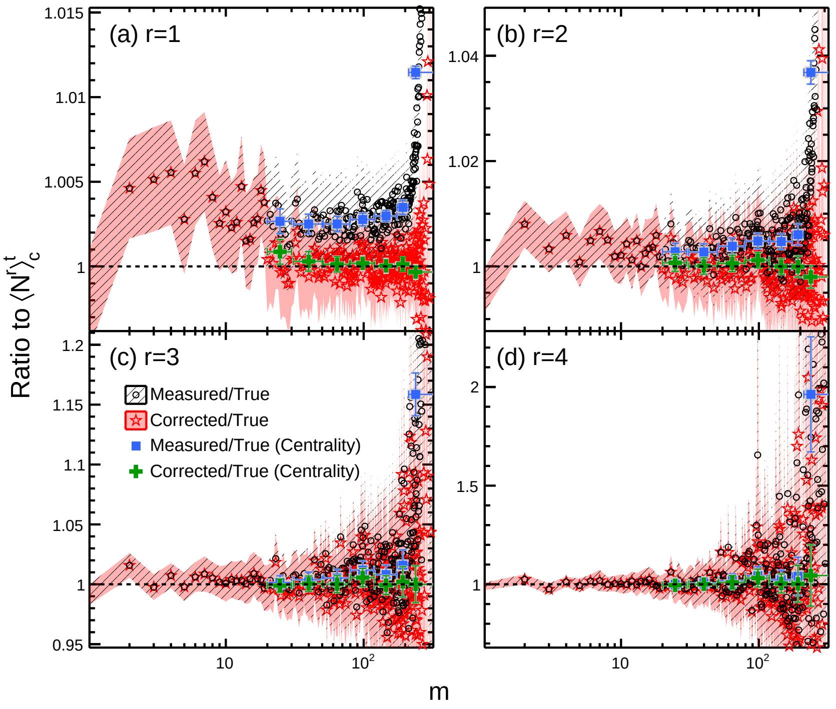

FIG. 7. The ratios of measured (black circles) and corrected (red stars) cumulants with respect to the true cumulants as functions of multiplicity. The bands represent the statistical uncertainties. The results averaged into 0-5, 5-10, 10-20,... and 50-60% centralities are shown in blue squares and green crosses.

B. Correction parameters

The new method relies on the probabilities $w_{i,j}$ and α_m, and other terms are all extracted from data. Hence, the systematic uncertainties would come from how precisely those parameters are determined in the simulations.

To check how the uncertainty of $w_{i,j}$ and α_m affects the final result, we again employ the model in Sec. III C and perform the pileup correction using wrong pileup probabilities, $\alpha(1 + p)$, with $\alpha = 0.05$. We vary the value of p from -10% to 10% and determine the values of $w_{i,j}$ and α_m according to Eqs. 5 and 6. The pileup correction is then performed with these wrong probabilities. Figure 8 shows cumulants up to the 4th order at 0-5% centrality as functions of p. It can be found that the results are overcorrected for $p > 0$, while the corrections are not enough for

$p < 0$. Further, higher-order cumulants get more affected by wrong values of the correction parameters as seen in the larger slope of the fitted functions. We would propose to consider those variations as systematic uncertainties on final results.

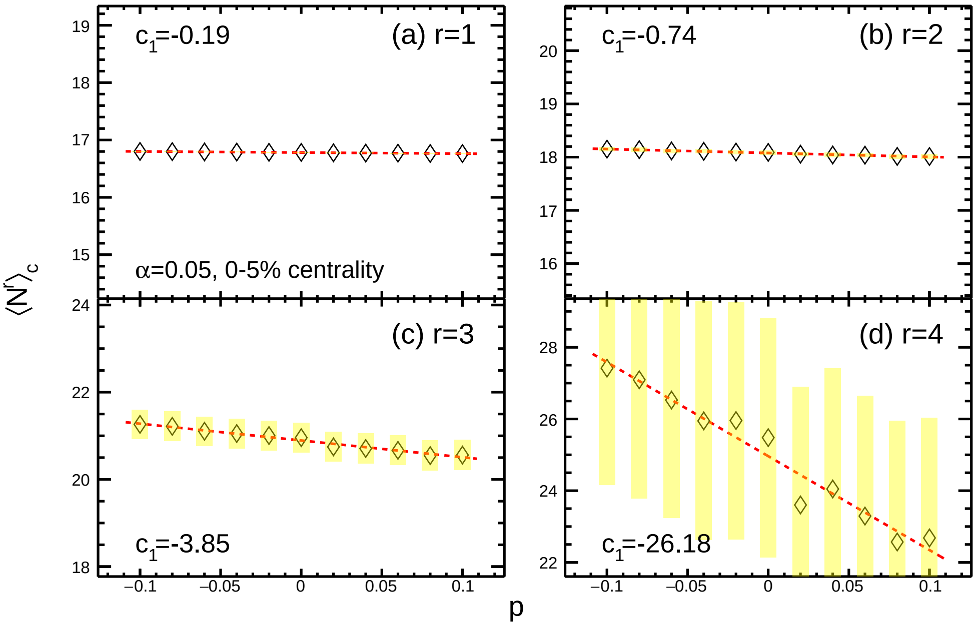

FIG. 8. Cumulants up to the 4th-order corrected with a wrong pileup probability , $\alpha(1+p)$, as a function of p. Statistical uncertainties are shown in bands. The red dotted lines are the polynomial fit functions with $c_1p + c_0$. The values of the fit parameter c_1 are shown in the panel. The scale of y-axis is set to ±15% with respect to the cumulant values at $p = 0$ for all panels.

V. SUMMARY

In this paper, we proposed a method to correct the effect of the pileup events on the higher-order moments and cumulants. The method can be derived by decomposing pileups into various combinations of sub-pileup events in terms of moments. The moments for sub-pileup events can be reconstructed assuming that the pileups are the consequences of the superposition between two independent events. We utilized the fact that the pileup changes the total multiplicity. The correction formulas are expressed by the sub-pileup moments and the moments from the lower multiplicity events, thus solvable from the lowest multiplicity events. Two models are performed with the same mean values of particle distributions for all multiplicity events, and with the $N_{\rm part}$-dependent mean values. The method works correctly for both cases. The method can deal with the pileup events for more than two single-collisions. The effect of trigger inefficiencies needs to be carefully checked by changing the starting point of the recursive corrections. The systematic uncertainties will be reduced by determining the pileup probability precisely.

Finally, we remark that one has to make sure that the detector efficiencies are corrected in a proper way [24–35] before performing the pileup correction.

VI. ACKNOWLEDGEMENT

This work was supported by Ito Science Foundation (2017) and JSPS KAKENHI Grant No. 25105504, 17K05442 and 19H05598.

---

[1] M. Bluhm *et al.*, Dynamics of critical fluctuations: Theory – phenomenology – heavy-ion collisions, (2020), arXiv:2001.08831 [nucl-th].
[2] S. Ejiri, F. Karsch, and K. Redlich, Hadronic fluctuations at the QCD phase transition, Phys. Lett. **B633**, 275 (2006), arXiv:hep-ph/0509051 [hep-ph].
[3] M. A. Stephanov, Non-Gaussian fluctuations near the QCD critical point, Phys. Rev. Lett. **102**, 032301 (2009), arXiv:0809.3450 [hep-ph].

[4] M. Asakawa, S. Ejiri, and M. Kitazawa, Third moments of conserved charges as probes of QCD phase structure, Phys. Rev. Lett. **103**, 262301 (2009), arXiv:0904.2089 [nucl-th].

[5] B. Friman, F. Karsch, K. Redlich, and V. Skokov, Fluctuations as probe of the QCD phase transition and freeze-out in heavy ion collisions at LHC and RHIC, Eur. Phys. J. **C71**, 1694 (2011), arXiv:1103.3511 [hep-ph].

[6] M. Arslandok, Recent results on net-baryon fluctuations in ALICE, in *28th International Conference on Ultrarelativistic Nucleus-Nucleus Collisions (Quark Matter 2019) Wuhan, China, November 4-9, 2019* (2020) arXiv:2002.03906 [nucl-ex].

[7] J. Adamczewski-Musch *et al.* (HADES), Proton number fluctuations in $\sqrt{s_{NN}} = 2.4$ GeV Au+Au collisions studied with HADES, (2020), arXiv:2002.08701 [nucl-ex].

[8] M. Mackowiak-Pawlowska (NA61/SHINE), NA61/SHINE results on fluctuations and correlations at CERN SPS energies, in *28th International Conference on Ultrarelativistic Nucleus-Nucleus Collisions (Quark Matter 2019) Wuhan, China, November 4-9, 2019* (2020) arXiv:2002.04847 [nucl-ex].

[9] M. M. Aggarwal *et al.* (STAR), Higher Moments of Net-proton Multiplicity Distributions at RHIC, Phys. Rev. Lett. **105**, 022302 (2010), arXiv:1004.4959 [nucl-ex].

[10] L. Adamczyk *et al.* (STAR), Beam energy dependence of moments of the net-charge multiplicity distributions in Au+Au collisions at RHIC, Phys. Rev. Lett. **113**, 092301 (2014), arXiv:1402.1558 [nucl-ex].

[11] L. Adamczyk *et al.* (STAR), Energy Dependence of Moments of Net-proton Multiplicity Distributions at RHIC, Phys. Rev. Lett. **112**, 032302 (2014), arXiv:1309.5681 [nucl-ex].

[12] L. Adamczyk *et al.* (STAR), Collision Energy Dependence of Moments of Net-Kaon Multiplicity Distributions at RHIC, (2017), arXiv:1709.00773 [nucl-ex].

[13] J. Adam *et al.* (STAR), Net-proton number fluctuations and the Quantum Chromodynamics critical point, (2020), arXiv:2001.02852 [nucl-ex].

[14] T. Nonaka (STAR), Measurement of the Sixth-Order Cumulant of Net-Proton Distributions in Au+Au Collisions from the STAR Experiment (2020) arXiv:2002.12505 [nucl-ex].

[15] M. Stephanov, On the sign of kurtosis near the QCD critical point, Phys. Rev. Lett. **107**, 052301 (2011), arXiv:1104.1627 [hep-ph].

[16] B. Friman, C. Hohne, J. Knoll, S. Leupold, J. Randrup, R. Rapp, and P. Senger, eds., *The CBM physics book: Compressed baryonic matter in laboratory experiments*, Vol. 814 (2011).

[17] H. Sako *et al.*, White paper for a Future J-PARC Heavy-Ion Program (J-PARC-HI), `http://asrc.jaea.go.jp/soshiki/gr/hadron/jparc-hi/`.

[18] S. Sombun, J. Steinheimer, C. Herold, A. Limphirat, Y. Yan, and M. Bleicher, Higher order net-proton number cumulants dependence on the centrality definition and other spurious effects, J. Phys. **G45**, 025101 (2018), arXiv:1709.00879 [nucl-th].

[19] P. Garg and D. Mishra, Higher moments of net-proton multiplicity distributions in a heavy-ion event pile-up scenario, Phys. Rev. C **96**, 044908 (2017), arXiv:1705.01256 [nucl-th].

[20] M. Asakawa and M. Kitazawa, Fluctuations of conserved charges in relativistic heavy ion collisions: An introduction, Prog. Part. Nucl. Phys. **90**, 299 (2016), arXiv:1512.05038 [nucl-th].

[21] X. Luo and N. Xu, Search for the QCD Critical Point with Fluctuations of Conserved Quantities in Relativistic Heavy-Ion Collisions at RHIC : An Overview, Nucl. Sci. Tech. **28**, 112 (2017), arXiv:1701.02105 [nucl-ex].

[22] V. Skokov, B. Friman, and K. Redlich, Volume Fluctuations and Higher Order Cumulants of the Net Baryon Number, Phys. Rev. **C88**, 034911 (2013), arXiv:1205.4756 [hep-ph].

[23] P. Braun-Munzinger, A. Rustamov, and J. Stachel, Bridging the gap between event-by-event fluctuation measurements and theory predictions in relativistic nuclear collisions, Nucl. Phys. **A960**, 114 (2017), arXiv:1612.00702 [nucl-th].

[24] A. Bialas and R. B. Peschanski, Moments of Rapidity Distributions as a Measure of Short Range Fluctuations in High-Energy Collisions, Nucl. Phys. **B273**, 703 (1986).

[25] M. Kitazawa and M. Asakawa, Revealing baryon number fluctuations from proton number fluctuations in relativistic heavy ion collisions, Phys. Rev. C **85**, 021901 (2012), arXiv:1107.2755 [nucl-th].

[26] M. Kitazawa and M. Asakawa, Relation between baryon number fluctuations and experimentally observed proton number fluctuations in relativistic heavy ion collisions, Phys. Rev. **C86**, 024904 (2012), [Erratum: Phys. Rev.C86,069902(2012)], arXiv:1205.3292 [nucl-th].

[27] A. Bzdak and V. Koch, Acceptance corrections to net baryon and net charge cumulants, Phys. Rev. **C86**, 044904 (2012), arXiv:1206.4286 [nucl-th].

[28] A. Bzdak and V. Koch, Local Efficiency Corrections to Higher Order Cumulants, Phys. Rev. **C91**, 027901 (2015), arXiv:1312.4574 [nucl-th].

[29] X. Luo, Unified Description of Efficiency Correction and Error Estimation for Moments of Conserved Quantities in Heavy-Ion Collisions, Phys. Rev. **C91**, 034907 (2015), arXiv:1410.3914 [physics.data-an].

[30] M. Kitazawa, Efficient formulas for efficiency correction of cumulants, Phys. Rev. **C93**, 044911 (2016), arXiv:1602.01234 [nucl-th].

[31] A. Bzdak, R. Holzmann, and V. Koch, Multiplicity dependent and non-binomial efficiency corrections for particle number cumulants, Phys. Rev. **C94**, 064907 (2016), arXiv:1603.09057 [nucl-th].

[32] T. Nonaka, M. Kitazawa, and S. Esumi, More efficient formulas for efficiency correction of cumulants and effect of using averaged efficiency, Phys. Rev. **C95**, 064912 (2017), arXiv:1702.07106 [physics.data-an].

[33] M. Kitazawa and X. Luo, Properties and uses of factorial cumulants in relativistic heavy-ion collisions, Phys. Rev. **C96**, 024910 (2017), arXiv:1704.04909 [nucl-th].

[34] T. Nonaka, M. Kitazawa, and S. Esumi, A general procedure for detectorresponse correction of higher order cumulants, Nucl. Instrum. Meth. **A906**, 10 (2018), arXiv:1805.00279 [physics.data-an].

[35] S. Esumi and T. Nonaka, Reconstructing particle number distributions with convoluting volume fluctuations, (2020), arXiv:2002.11253 [physics.data-an].